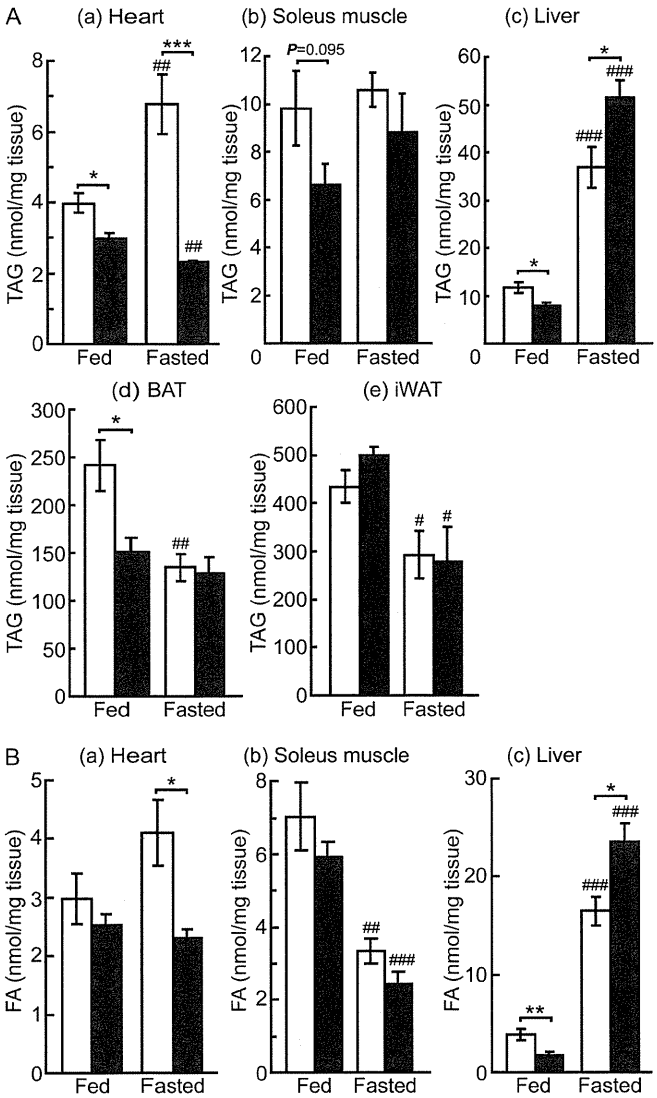


FIGURE 3. **TAG and FA contents in the tissues of fed and fasted wild-type and *Plin5*$^{-/-}$ mice.** *A*, TAG content in the heart (*panel a*), soleus muscle (*panel b*), liver (*panel c*), BAT (*panel d*), and inguinal WAT (*panel e*) ($n$ = 5–8 per group). *B*, free FA content in the heart (*panel a*), soleus muscle (*panel b*), and liver (*panel c*) ($n$ = 5–8 per group). *Open bars*, wild-type mice, and *filled bars*, *Plin5*$^{-/-}$ mice. ***, $p < 0.001$; **, $p < 0.01$; *, $p < 0.05$; ###, $p < 0.001$; ##, $p < 0.01$; #, $p < 0.05$, against fed animals of the same genotypes.

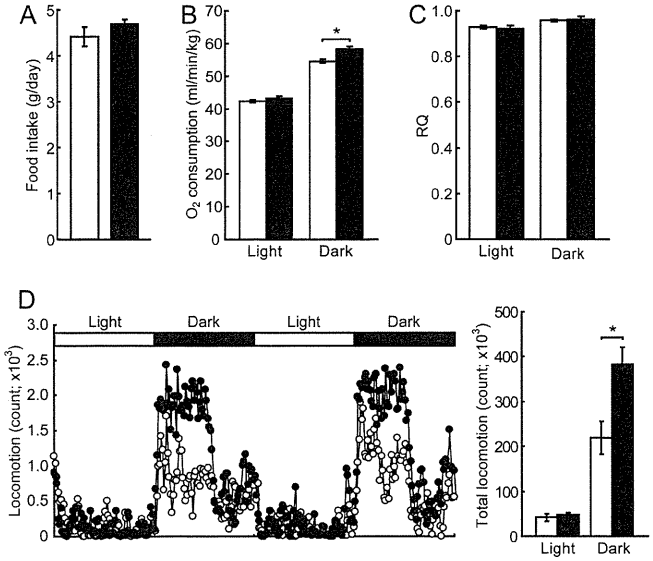


FIGURE 4. **Energy metabolism of *Plin5*$^{-/-}$ mice.** *A*, food intake. Mice were housed individually for 10 days, and food intake per day was measured ($n$ = 10 per group). *B*, oxygen consumption. *C*, respiratory quotient ($n$ = 6 per group). *D*, locomotion of *Plin5*$^{-/-}$ mice. Dot-plot demonstrates the time course of locomotor activity during 2 days. Each *dot* is the mean of locomotion of six mice. The *graph* on the *right* represents the total counts of locomotion during the experiment. *, $p < 0.05$.

ing wild-type mice, many of the particulates positive for Plin5 and Plin2 exhibited ring-shaped images typical of LDs (Fig. 6*D*). These structures were also positive for lipid staining with Bodipy (132 of 147 Plin5-positive particles being Bodipy-positive) (Fig. 6*F*). For fed wild-type mice, however, the particles were rarely ring-shaped (Fig. 6*C*) and mostly devoid of lipid staining (only 8 of 132 Plin5-positive particles being Bodipy-positive) (Fig. 6*E*). We obtained similar immunostaining patterns with another lot of anti-Plin5 antibody (data not shown). These results suggest that most of the particles carrying Plin5 and Plin2 in the hearts of fed wild-type mice represent very small LDs with low lipid contents. They are hardly detectable in conventional microscopy, because they are not stained with ORO. In the hearts of *Plin5*$^{-/-}$ mice, no LDs were detected by Bodipy staining (Fig. 6, *G* and *H*), but, interestingly, Plin2 still exhibited punctate staining irrespective of feeding conditions (Fig. 6, *I* and *J*).

We examined the effect of Plin5 ablation on the expression of other perilipin proteins and lipases. Among them, Plin2 protein expression in the heart was significantly decreased upon Plin5 ablation (Fig. 7*A*). However, expression of Plin2 mRNA was not significantly affected by Plin5 ablation (Fig. 7*B*), indicating the involvement of a post-transcriptional event in the decrease of Plin2 protein. Previous studies found Plin2 protein to be degraded by proteasomes under conditions where Plin2 was not stabilized by binding to LDs or lipids (29, 30). Thus, it is conceivable that Plin2 does not compensate for the ablation of Plin5 in supporting LDs to be detectable but is rather degraded to a large extent in the hearts of *Plin5*$^{-/-}$ mice. However, as suggested by immunofluorescence microscopy (Fig. 6, *I* and *J*), the remaining Plin2 was still located on particulate structures, even though LDs were undetectable by electron microscopy or lipid staining. mRNA expression of Plin3, ATGL, and HSL was slightly affected by Plin5 ablation (Fig. 7*B*), but their protein amounts did not differ between the two genotypes (Fig. 7*A*).

*Plin5 Maintains LDs by Restricting Lipase(s)*—Perilipin family proteins have generally been suggested to protect LDs from attack by lipases (17). Hence, we supposed that the apparent lack of LDs in the hearts of *Plin5*$^{-/-}$ mice is due to the loss of this function. To examine this notion, we tried to inhibit lipase(s), particularly ATGL, a major lipase of the heart, in the intact organ. For this purpose, the hearts of *Plin5*$^{-/-}$ mice were briefly perfused with BEL, a potent inhibitor of the iPLA$_2$ family of phospholipases/lipases, including ATGL (31). This treatment effectively eliminated the BEL-sensitive lipase activities in the heart in both genotypes of mice, as confirmed by an *in vitro* lipase assay (Fig. 8*A*). Importantly, the ratio of lipase activity remaining after the treatment in wild-type mice (70%) was

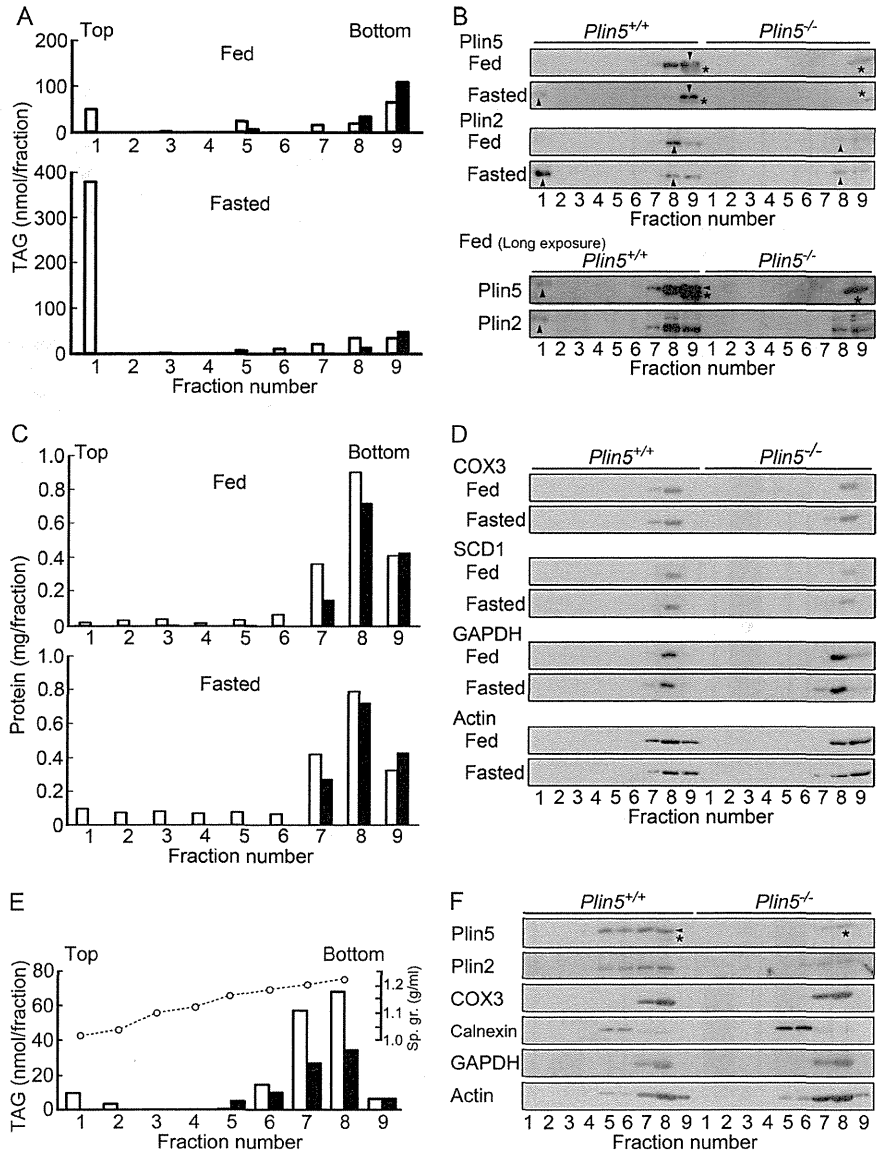


FIGURE 5. **Subcellular fractionation of heart homogenates.** *A*, TAG content in the fractions obtained by sucrose density gradient centrifugation of heart homogenates of wild-type and *Plin5*$^{-/-}$ mice under fed and fasted conditions. *Open bar*, wild-type mice, and *filled bar*, *Plin5*$^{-/-}$ mice. *B*, immunoblotting of Plin5 and Plin2 in the fractions of *A*. For fed animals, results of long exposure of the blots are also shown. *Arrowhead*, Plin5 and Plin2. *Asterisk*, nonspecific band, which was not recognized by another lot of anti-Plin5 antibody (Progen) raised against the same carboxyl-terminal epitope. *C*, protein contents in the same fractions. *D*, distribution of markers of mitochondria (cytochrome *c* oxidase subunit 3 (*COX3*)), endoplasmic reticulum (stearoyl-CoA desaturase 1 (*SCD1*)), and cytosol (glyceraldehyde-3-phosphate dehydrogenase (*GAPDH*)), and actin filament through the gradients. *E*, TAG content in the fractions after centrifugation through a wider sucrose-density gradient. Heart homogenates from fed wild-type (*open bar*) and *Plin5*$^{-/-}$ (*filled bar*) mice were analyzed. *Open circle*, specific gravity (*Sp. gr.*) of each fraction. *F*, distribution of Plin5, Plin2, and marker proteins in the same fractions as in *E*. Calnexin was used as a marker of endoplasmic reticulum.

comparable with the ratio of remaining heart lipase activity in ATGL-KO mice (23). Interestingly, the BEL-sensitive lipase activity was significantly lower in the hearts of *Plin5*$^{-/-}$ mice than that of wild-type mice, despite the similar ATGL protein level in both genotypes of mice (Fig. 7*A*). After BEL perfusion, LDs were observed in the hearts of *Plin5*$^{-/-}$ mice as abundantly as in wild-type mice (Fig. 8*B*). The amount of Plin2 relative to that of an internal control, GAPDH, was also recovered by the perfusion, to a level close to that in wild-type mice (Fig. 8*C*). Moreover, the TAG content in the hearts of *Plin5*$^{-/-}$ mice was increased by the treatment, reaching a level indistinguishable from that of wild-type mice without the inhibitor (Fig. 8*D*). Thus, detectable LDs as well as lipid accumulation was recovered by inhibiting ATGL and related lipases in the hearts of *Plin5*$^{-/-}$ mice. This result indicates that Plin5 maintains LDs in the heart by blocking the actions of ATGL and possibly other lipase(s).

*Plin5 Deficiency Promotes Fatty Acid Oxidation in Cardiomyocytes*—We next asked how FA is managed in the hearts of *Plin5*$^{-/-}$ mice, where it is poorly sequestered as TAG. To address this issue, FA oxidation was monitored with cultured cardiomyocytes. For convenience, hearts from mice 1.5–3 days after birth, in which Plin5 and FA oxidation enzymes were fully expressed (Fig. 9*A*), were used. Expression of those

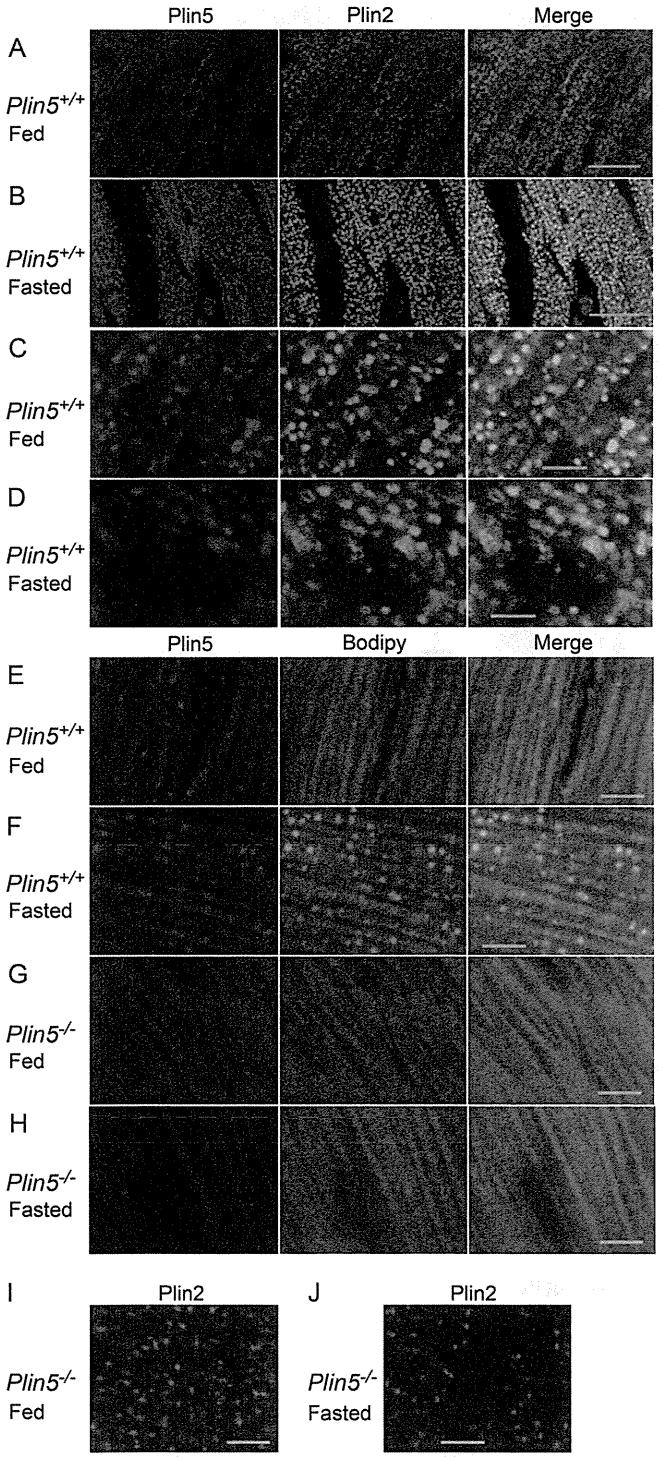


FIGURE 6. **Immunofluorescence staining of heart sections.** *A–D*, immunofluorescence staining of Plin5 and Plin2 in heart sections from wild-type mice. *A* and *C*, fed mice; and *B* and *D*, starved mice. *A* and *B*, low magnification. *Bar*, 20 μm. *C* and *D*, high magnification. *Bar*, 5 μm. *E–H*, double staining with an anti-Plin5 antibody and Bodipy 493/503. Cryosections of the hearts of wild-type (*E* and *F*) and *Plin5*$^{-/-}$ (*G* and *H*) mice under fed (*E* and *G*) and fasted (*F* and *H*) conditions were stained. *I* and *J*, immunostaining of Plin2 in *Plin5*$^{-/-}$ mice under fed (*I*) and fasted (*J*) conditions. *Bar*, 5 μm.

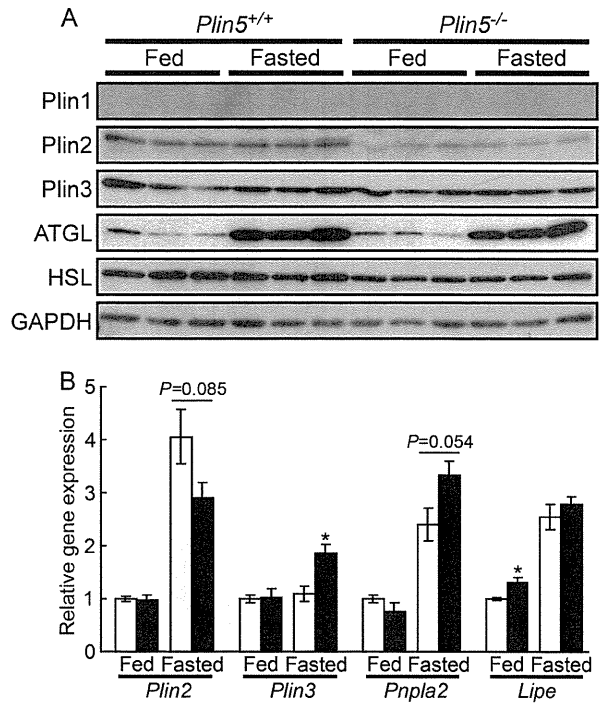


FIGURE 7. **Expression of perilipin family proteins and lipases in the heart.** *A*, immunoblotting of the proteins (three animals for each group). *B*, quantitative RT-PCR of mRNAs. Signal intensities were corrected based on that of *Rplp0* (36B4) ($n = 5$ per group). *Open bar*, wild-type mice, and *filled bar*, *Plin5*$^{-/-}$ mice. *, $p < 0.05$, against wild-type mice under the same feeding condition. *Pnpla2* and *Lipe* denote the genes of ATGL and HSL, respectively.

proteins and lipases was largely retained during the culture (Fig. 9*B*). In *Plin5*$^{-/-}$ cells, the radioactivity of palmitic acid was significantly better incorporated into $CO_2$ (Fig. 9*C*). Production of intracellular ASM (Fig. 9*D*), which represent active metabolites such as acetyl-CoA and tricarboxylic acid cycle intermediates (32), was also increased in *Plin5*$^{-/-}$ cells. However, radioactivity in extracellular ASM, probably representing products excluded from active metabolism, was not changed by deletion of Plin5 (Fig. 9*E*). Etomoxir is a specific inhibitor of carnitine *O*-palmitoyltransferase type 1, an enzyme required for the translocation of fatty acyl-CoA into mitochondria. This agent significantly, albeit partially, inhibited the production of radioactive $CO_2$ and intracellular ASM (Fig. 9, *C* and *D*). It was reported that in the mice intraperitoneally injected with etomoxir, CPT1 activity was decreased only by 40% in the heart and nearly completely in the liver and skeletal muscle (33), although the reason was not defined. Thus, it is conceivable that mitochondria make a major contribution to FA oxidation in this experimental setting, although the contribution of peroxisomal FA oxidation activity would not be neglected. Total incorporation of FA was not different between *Plin5*$^{-/-}$ and wild-type cells (Fig. 9*F*). Thus, impaired TAG accumulation in the hearts of *Plin5*$^{-/-}$ mice is not due to decreased uptake of FA. Taken together, these results suggest that FA is rapidly oxidized in mitochondria in the hearts of *Plin5*$^{-/-}$ mice, rather than being retained as TAG.

*Plin5 Deficiency Increases Oxidative Stress to the Heart*—Enhanced fatty acid oxidation may lead to increased production of ROS (34), a mediator of lipotoxicity. Accordingly, we estimated ROS production in the hearts of wild-type and *Plin5*$^{-/-}$ mice by measuring the content of lipid peroxide, a product of peroxidative action by ROS. The level of lipid peroxide was signifi-

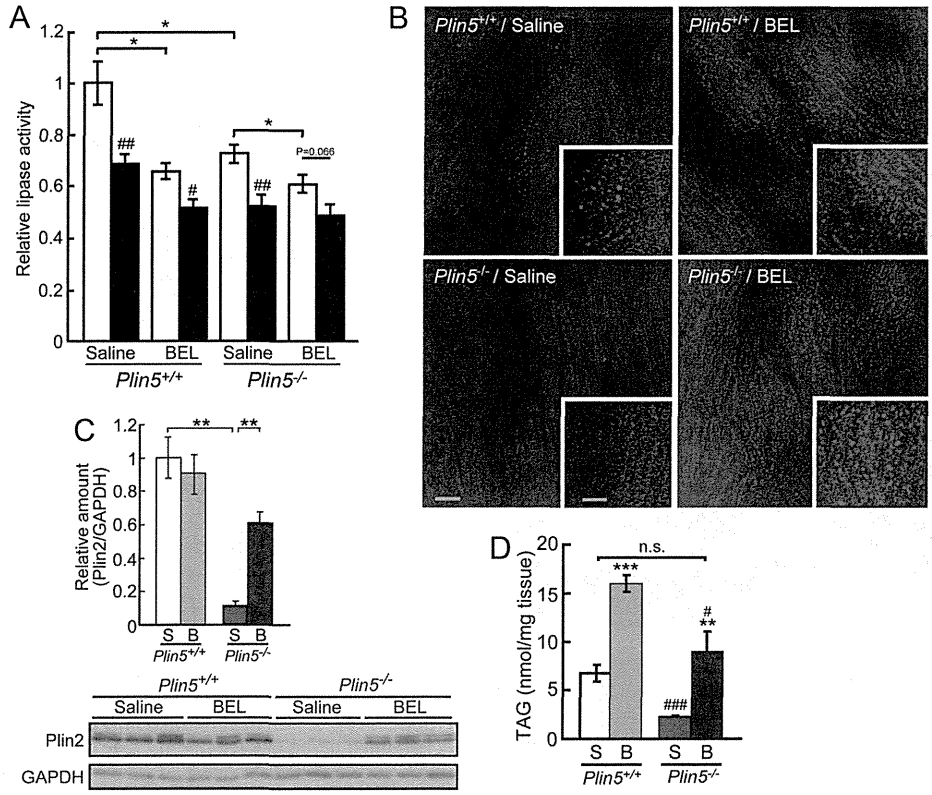


FIGURE 8. **Plin5 maintains LDs by restricting lipases.** *A*, decrease in heart lipase activities by the perfusion with BEL. Lipase activities were measured with the heart homogenates of mice perfused with saline or BEL ($n = 3–4$ per group). Assays were performed in the absence (*open bar*) or presence (*filled bar*) of 50 μM BEL. Relative enzyme activities taking the value of saline-treated wild-type mice measured without BEL (14.1 nmol of oleic acid released/h/mg of protein) as 1. *, $p < 0.05$; ##, $p < 0.01$; #, $p < 0.05$, against values obtained without BEL during the assay for the same genotypes of mice with the same treatment. *B*, effect of BEL perfusion on the occurrence of LDs in the hearts of wild-type and *Plin5*$^{-/-}$ mice. Representative images of Nile Red-stained frozen sections are shown. *Bar*, 10 μm. *Inset*, high magnification view. *Bar*, 5 μm. Results were confirmed for several microscopic fields obtained from at least two animals for each group. *C*, effect of BEL on the protein content of Plin2 in the heart. *Top*, relative amount of Plin2 normalized with that of GAPDH in the heart lysates from the same animals as in *A* ($n = 3$), estimated from the result of immunoblotting (*bottom*). *S*, saline-treated, and *B*, BEL-treated. **, $p < 0.01$. *D*, effect of BEL on TAG content in the heart ($n = 5–8$ per group). ***, $p < 0.001$; **, $p < 0.01$, against saline-treated animals of the same genotype. ###, $p < 0.001$; #, $p < 0.05$, against wild-type mice with the same treatment. *n. s.*, difference not significant.

cantly higher in the hearts of *Plin5*$^{-/-}$ mice than that of wild-type mice at both 16–20 and 30–38 weeks of age, although the values increased with age in both genotypes (Fig. 10*A*). NAC is a precursor of glutathione, a substrate for glutathione peroxidase, and is often used to alleviate oxidative stress (35). The mice were continuously given this agent from 16 to 18 weeks to the day of experiment at 30–32 weeks of age. By this treatment, the heart content of lipid peroxide was lowered in *Plin5*$^{-/-}$ mice to a level close to that of younger wild-type mice. This result indicates that NAC indeed counteracted the increased action of ROS in the hearts of *Plin5*$^{-/-}$ mice in this experimental setting.

The increase in oxidative stress may affect the contractile function of the hearts of *Plin5*$^{-/-}$ mice. This possibility was examined by echocardiography, using mice 16–18 and 30–38 weeks old (Fig. 10*B*). End-diastolic dimension (LVID;d) and end-systolic dimension (LVID;s) were enlarged, and FS was reduced in the aged *Plin5*$^{-/-}$ mice but not in wild-type mice (Fig. 10*C*). These values returned to normal in the aged *Plin5*$^{-/-}$ mice on treatment with NAC from 16 to 18 to 30–32 weeks. In the regression analysis for the aged mice, lipid peroxide levels in the hearts of individual animals correlated well with LVID;d and LVID;s and moderately with FS (Fig. 10*D*). The correlation between FS and the lipid peroxide level was apparently lower, because FS was derived from LVID;d and LVID;s by calculation, which unavoidably expands variations. Hence, ablation of Plin5 leads to further weakening of heart function with age, and the cumulative effects of increased oxidative stress are likely to contribute to this.

## DISCUSSION

One of the most striking observations from *Plin5*$^{-/-}$ mice is that *Plin5*$^{-/-}$ mice lacked detectable LDs only in the heart. Consistent with the apparent lack of LDs, the hearts of *Plin5*$^{-/-}$ mice contained significantly less TAG and FA, as compared with that of wild-type mice. LDs were recovered upon brief perfusion of the heart with an inhibitor of ATGL and related lipases. This result indicates that Plin5 antagonizes lipase actions, consistent with observations that perilipin family members, including Plin5, protect TAG from attack by lipases (5, 6, 17). Several recent reports (28, 36) suggested that Plin5 serves as a platform for the interaction of ATGL with CGI-58 on the LD surface, thus facilitating lipolysis. Another group reported that Plin5 interacts with ATGL and inhibits the enzymatic activity (37). Data from this study suggest that the func-

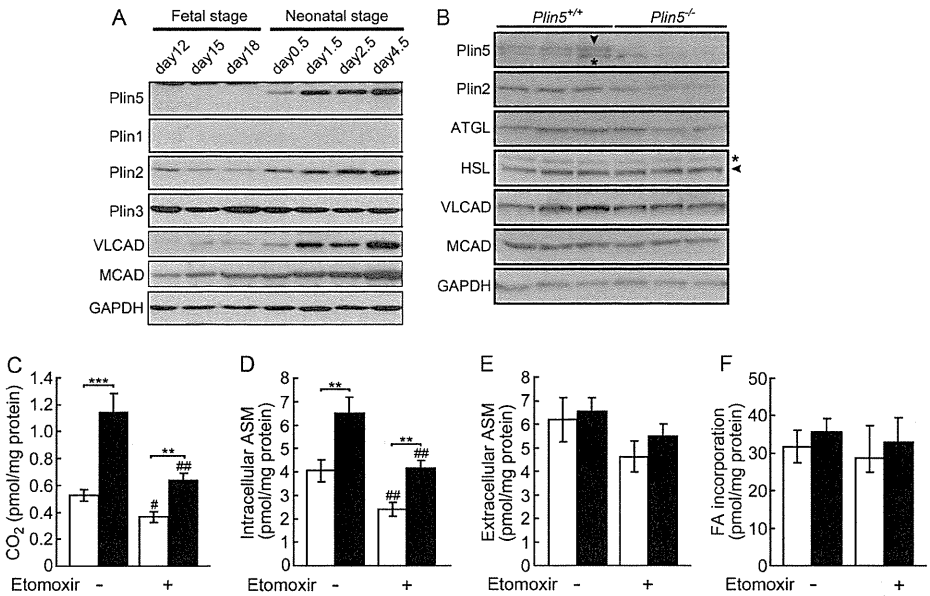


FIGURE 9. **Lack of Plin5 promotes FA oxidation in cardiomyocytes.** *A*, expression of perilipin family proteins and fatty acid oxidation enzymes in the hearts of wild-type mice before and after birth. *VLCAD*, very long-chain acyl-CoA dehydrogenase, and *MCAD*, medium-chain acyl-CoA dehydrogenase. *B*, expression of perilipin family proteins, lipases, and fatty acid-oxidizing enzymes in cardiomyocytes after the culture for 2 days in the presence of oleic acid (see "Experimental Procedures"). Cardiomyocytes prepared from the hearts of eight wild-type and *Plin5*$^{-/-}$ mice 3 days after birth were seeded in three culture dishes, respectively. *Arrowhead*, correct band of Plin5 and HSL. *, nonspecific band. *C–E*, FA oxidation by cardiomyocytes as assessed by conversion of [$^{14}$C]palmitic acid to $CO_2$ (*C*), intracellular ASM (*D*), and extracellular ASM (*E*). *F*, total incorporation of FA. *Open bar*, wild-type mice, and *filled bar*, *Plin5*$^{-/-}$ mice. The assay was performed with or without etomoxir. $n = 8–9$ representing the number of independent experiments per group. In each experiment, values obtained with three culture dishes were averaged. ***, $p < 0.001$; **, $p < 0.01$; ##, $p < 0.01$; #, $p < 0.05$, against etomoxir-untreated cells of the same genotype.

tion of Plin5 in the heart is to impede, rather than assist, lipolysis.

LDs were observed in other tissues, including skeletal muscle, the liver, BAT, and WAT of *Plin5*$^{-/-}$ mice. The content of TAG was decreased in the liver and BAT of fed *Plin5*$^{-/-}$ mice, as compared with wild-type mice. Interestingly, in the fasted state, the liver of *Plin5*$^{-/-}$ mice contained more TAG and FA than that of wild-type mice, in contrast to the case of the heart. These results suggest that roles of Plin5 as well as LDs may differ, depending on the functions of individual cell and tissue types. It is also possible that the unique combinations of Plin5 with other LD proteins, including the perilipin family members, confer tissue-specific function. Plin5 is more protective than Plin2, another major perilipin protein in the heart, according to previous observations (37, 38). We also confirmed it by an experiment in which we expressed Plin5 or Plin2, with or without ATGL, in cultured cells (data not shown). The protective function of Plin5 in the heart is not substituted for by other proteins, including Plin2, probably due to highly active lipid metabolism. In fact, the resting metabolic rate on a fat-free mass basis is much higher in the heart than in most other organs, including skeletal muscle and the liver (39). Moreover, 60–70% of energy is supplied by FA in the heart (20). Thus, at least under sedentary conditions, lipid metabolism is more moderate in tissues other than the heart. Hence, other proteins may effectively compensate for a deficiency of Plin5 to maintain detectable LDs in those tissues.

In this study, the occurrence of very small LDs in the hearts of fed wild-type mice was suggested by immunofluorescence microscopy and subcellular fractionation. These structures seem to be under the limit of detection with ORO or Bodipy, because of their small size and low lipid content. They would not float, but rather sediment, upon centrifugation under the usual conditions for LD isolation, due to their higher protein to lipid ratio. A precedent of dense protein-lipid complex is plasma high density lipoprotein. Its density ranges 1.063–1.210 (40), overlapping the density 1.09–1.10 at the bottom in the present fractionation experiment (Fig. 5, *A* and *B*). We confirmed that they are indeed structures with defined densities by a centrifugal experiment employing a wider range of sucrose gradients (Fig. 5, *E* and *F*).

Plin5 and Plin2 did not seem to coat LDs evenly in immunofluorescence microscopy of the heart. In subcellular fractionation, Plin5 tended to be less concentrated in the upper fractions, and more abundant in the lower fractions, particularly the pellet, as compared with Plin2. Thus, Plin5 seems to be more abundant in smaller LDs as compared with Plin2. Occurrence of immature LDs abundant in Plin5 in cultured cells as well as the heart and liver was reported very recently (41). Thus, it is conceivable that Plin5 is particularly important for protecting very small LDs that have larger relative surface areas from lipase attack. Involvement of Plin5 in the interaction between LDs and mitochondria was shown recently (42). In this cell fractionation study, the distribution of Plin5 partially overlapped that of mitochondria, possibly being consistent with the report.

In the hearts of *Plin5*$^{-/-}$ mice, Plin2 exhibited a punctate distribution in immunofluorescence microscopy. Moreover, TAG was mostly recovered, and Plin2 was also to a large extent recovered in the pellet by subcellular fractionation (Fig. 5, *A* and *B*). Thus, it is conceivable that, Plin2-coated minute LDs still occur in the hearts of *Plin5*$^{-/-}$ mice, despite the apparent lack

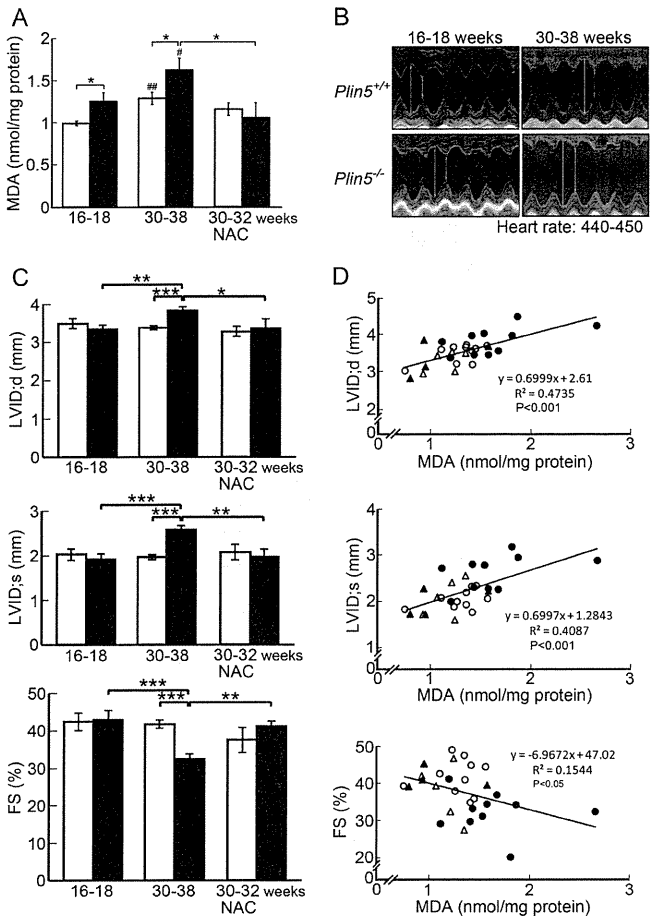


FIGURE 10. **Plin5 deficiency enhances oxidative burden in the heart, causing a functional decline.** *A*, evaluation of ROS generation by TBARS assay. Malondialdehyde (*MDA*) was quantified colorimetrically to monitor lipid peroxidation. Measurements were performed on the hearts from mice at 16–18 weeks ($n = 9$), 30–38 weeks ($n = 10$), and mice continuously treated with NAC from 16 to 18 weeks of age to the day of the experiment at 30–32 weeks of age ($n = 5$ for wild-type and 4 for *Plin5*$^{-/-}$ mice, respectively). *B*, representative images of echocardiography in age-matched mice (16–18 or 30–38 weeks old). *Long* and *short vertical lines* indicate LVID;d and LVID;s, respectively. *C*, values of LVID;d (*top panel*), LVID;s (*middle panel*), and FS (*bottom panel*) were evaluated from images of echocardiography, at heart rates of 440–450 beats/min. $n = 6$ for both genotypes at 16–18 weeks, 23 and 16 for wild-type and *Plin5*$^{-/-}$ mice at 30–38 weeks, respectively, and 5 and 4 for NAC-treated wild-type and *Plin5*$^{-/-}$ mice, respectively. *Open bar*, wild-type mice, and *filled bar*, *Plin5*$^{-/-}$ mice. ***, $p < 0.001$; **, $p < 0.01$; *, $p < 0.05$; ##, $p < 0.01$; #, $p < 0.05$, against the values of young mice of the same genotype. *D*, regression analysis of the correlations between the heart MDA content and LVID;d (*top panel*), LVID;s (*middle panel*), and FS (*bottom panel*). The first-order regression line was obtained by the least squares method from the data for individual mice. *Open* and *closed circles*, wild-type and *Plin5*$^{-/-}$ mice at 30–38 weeks, and *open* and *closed triangles*, NAC-treated wild-type and *Plin5*$^{-/-}$ mice, respectively.

of LDs. They are under the limit of detection by usual microscopic techniques, due to their small sizes. They are largely, but probably not completely, depleted of TAG due to the absence of Plin5. Hence, most, if not all, of TAG remaining in the hearts of *Plin5*$^{-/-}$ mice is conceivably accommodated in those minute LDs. TAG may also be retained in part in other cellular compartments such as mitochondria and endoplasmic reticulum, as suggested by a classical study (43). A recent finding also showed that TAG is even an intrinsic component of an enzyme complex, cytochrome *c* oxidase (44).

The *Plin5*$^{-/-}$ mice allow one to evaluate the physiological significance of LDs in the heart. The generation of ROS was significantly promoted in the hearts of *Plin5*$^{-/-}$ mice, as assessed by the elevated level of lipid peroxide. This is consistent with the enhanced mitochondrial oxidation of FA in *Plin5*$^{-/-}$ mice; $FADH_2$ generated during the β-oxidation of FA promotes the production of ROS, by reversing the electron flow from mitochondrial complex II to complex I, a major site of ROS production (34). It is widely recognized that ROS induce cardiac hypertrophy and cardiomyocyte dysfunction through oxidative damage and/or aberrant redox signaling (45). In echocardiography, *Plin5*$^{-/-}$ mice exhibited a greater decrease in heart function at older ages, as compared with wild-type mice. Continuous NAC treatment negated this, as well as lowered the level of lipid peroxide. Moreover, the heart parameters significantly correlated with lipid peroxide levels on an individual basis. Based on these results, we propose that an important function of Plin5 in the heart is to suppress excess ROS production by sequestering FA in TAG, thus reducing FA oxidation in mitochondria. This function is crucial for protecting the heart from eventual functional decline.

*Acknowledgments—We thank Drs. R. Zechner and T. Koide for critical reading of the manuscript. We also thank Drs. Takashi Hashimoto and S. Yamaguchi for anti-VLCAD and anti-MCAD antibodies and Dr. J. Suzuki for technical advice on the TBARS assay.*

## REFERENCES

1. Schaffer, J. E. (2003) Lipotoxicity. When tissues overeat. *Curr. Opin. Lipidol.* **14,** 281–287
2. Brasaemle, D. L. (2007) Thematic review series. Adipocyte biology. The perilipin family of structural lipid droplet proteins. Stabilization of lipid droplets and control of lipolysis. *J. Lipid Res.* **48,** 2547–2559
3. Kimmel, A. R., Brasaemle, D. L., McAndrews-Hill, M., Sztalryd, C., and Londos, C. (2010) Adoption of perilipin as a unifying nomenclature for the mammalian PAT family of intracellular lipid storage droplet proteins. *J. Lipid Res.* **51,** 468–471
4. Yamaguchi, T., Matsushita, S., Motojima, K., Hirose, F., and Osumi, T. (2006) MLDP, a novel PAT family protein localized to lipid droplets and enriched in the heart, is regulated by peroxisome proliferator-activated receptor α. *J. Biol. Chem.* **281,** 14232–14240
5. Wolins, N. E., Quaynor, B. K., Skinner, J. R., Tzekov, A., Croce, M. A., Gropler, M. C., Varma, V., Yao-Borengasser, A., Rasouli, N., Kern, P. A., Finck, B. N., and Bickel, P. E. (2006) OXPAT/PAT-1 is a PPAR-induced lipid droplet protein that promotes fatty acid utilization. *Diabetes* **55,** 3418–3428
6. Dalen, K. T., Dahl, T., Holter, E., Arntsen, B., Londos, C., Sztalryd, C., and Nebb, H. I. (2007) LSDP5 is a PAT protein specifically expressed in fatty acid-oxidizing tissues. *Biochim. Biophys. Acta* **1771,** 210–227
7. Martinez-Botas, J., Anderson, J. B., Tessier, D., Lapillonne, A., Chang, B. H., Quast, M. J., Gorenstein, D., Chen, K. H., and Chan, L. (2000) Absence of perilipin results in leanness and reverses obesity in Lepr(db/db) mice. *Nat. Genet.* **26,** 474–479
8. Tansey, J. T., Sztalryd, C., Gruia-Gray, J., Roush, D. L., Zee, J. V., Gavrilova, O., Reitman, M. L., Deng, C. X., Li, C., Kimmel, A. R., and Londos, C. (2001) Perilipin ablation results in a lean mouse with aberrant adipocyte lipolysis, enhanced leptin production, and resistance to diet-induced obesity. *Proc. Natl. Acad. Sci. U.S.A.* **98,** 6494–6499
9. Sztalryd, C., Xu, G., Dorward, H., Tansey, J. T., Contreras, J. A., Kimmel, A. R., and Londos, C. (2003) Perilipin A is essential for the translocation of hormone-sensitive lipase during lipolytic activation. *J. Cell Biol.* **161,** 1093–1103
10. Lass, A., Zimmermann, R., Haemmerle, G., Riederer, M., Schoiswohl, G., Schweiger, M., Kienesberger, P., Strauss, J. G., Gorkiewicz, G., and Zech-

ner, R. (2006) Adipose triglyceride lipase-mediated lipolysis of cellular fat stores is activated by CGI-58 and defective in Chanarin-Dorfman syndrome. *Cell Metab.* **3,** 309–319
11. Yamaguchi, T., Omatsu, N., Morimoto, E., Nakashima, H., Ueno, K., Tanaka, T., Satouchi, K., Hirose, F., and Osumi, T. (2007) CGI-58 facilitates lipolysis on lipid droplets but is not involved in the vesiculation of lipid droplets caused by hormonal stimulation. *J. Lipid Res.* **48,** 1078–1089
12. Miyoshi, H., Perfield, J. W., 2nd, Souza, S. C., Shen, W. J., Zhang, H. H., Stancheva, Z. S., Kraemer, F. B., Obin, M. S., and Greenberg, A. S. (2007) Control of adipose triglyceride lipase action by serine 517 of perilipin A globally regulates protein kinase A-stimulated lipolysis in adipocytes. *J. Biol. Chem.* **282,** 996–1002
13. Shen, W. J., Patel, S., Miyoshi, H., Greenberg, A. S., and Kraemer, F. B. (2009) Functional interaction of hormone-sensitive lipase and perilipin in lipolysis. *J. Lipid Res.* **50,** 2306–2313
14. Granneman, J. G., Moore, H. P., Krishnamoorthy, R., and Rathod, M. (2009) Perilipin controls lipolysis by regulating the interactions of AB-hydrolase containing 5 (Abhd5) and adipose triglyceride lipase (Atgl). *J. Biol. Chem.* **284,** 34538–34544
15. Radner, F. P., Streith, I. E., Schoiswohl, G., Schweiger, M., Kumari, M., Eichmann, T. O., Rechberger, G., Koefeler, H. C., Eder, S., Schauer, S., Theussl, H. C., Preiss-Landl, K., Lass, A., Zimmermann, R., Hoefler, G., Zechner, R., and Haemmerle, G. (2010) Growth retardation, impaired triacylglycerol catabolism, hepatic steatosis, and lethal skin barrier defect in mice lacking comparative gene identification-58 (CGI-58). *J. Biol. Chem.* **285,** 7300–7311
16. Zechner, R., Kienesberger, P. C., Haemmerle, G., Zimmermann, R., and Lass, A. (2009) Adipose triglyceride lipase and the lipolytic catabolism of cellular fat stores. *J. Lipid Res.* **50,** 3–21
17. Bell, M., Wang, H., Chen, H., McLenithan, J. C., Gong, D. W., Yang, R. Z., Yu, D., Fried, S. K., Quon, M. J., Londos, C., and Sztalryd, C. (2008) Consequences of lipid droplet coat protein down-regulation in liver cells. Abnormal lipid droplet metabolism and induction of insulin resistance. *Diabetes* **57,** 2037–2045
18. Chang, B. H., Li, L., Paul, A., Taniguchi, S., Nannegari, V., Heird, W. C., and Chan, L. (2006) Protection against fatty liver but normal adipogenesis in mice lacking adipose differentiation-related protein. *Mol. Cell. Biol.* **26,** 1063–1076
19. Sztalryd, C., Bell, M., Lu, X., Mertz, P., Hickenbottom, S., Chang, B. H., Chan, L., Kimmel, A. R., and Londos, C. (2006) Functional compensation for adipose differentiation-related protein (ADFP) by Tip47 in an ADFP null embryonic cell line. *J. Biol. Chem.* **281,** 34341–34348
20. van der Vusse, G. J., van Bilsen, M., and Glatz, J. F. (2000) Cardiac fatty acid uptake and transport in health and disease. *Cardiovasc. Res.* **45,** 279–293
21. Bachmanov, A. A., Reed, D. R., Beauchamp, G. K., and Tordoff, M. G. (2002) Food intake, water intake, and drinking spout side preference of 28 mouse strains. *Behav. Genet.* **32,** 435–443
22. Bligh, E. G., and Dyer, W. J. (1959) A rapid method of total lipid extraction and purification. *Can. J. Biochem. Physiol.* **37,** 911–917
23. Haemmerle, G., Lass, A., Zimmermann, R., Gorkiewicz, G., Meyer, C., Rozman, J., Heldmaier, G., Maier, R., Theussl, C., Eder, S., Kratky, D., Wagner, E. F., Klingenspor, M., Hoefler, G., and Zechner, R. (2006) Defective lipolysis and altered energy metabolism in mice lacking adipose triglyceride lipase. *Science* **312,** 734–737
24. Nakamura, T. Y., Goda, K., Okamoto, T., Kishi, T., Nakamura, T., and Goshima, K. (1993) Contractile and morphological impairment of cultured fetal mouse myocytes induced by oxygen radicals and oxidants. Correlation with intracellular $Ca^{2+}$ concentration. *Circ. Res.* **73,** 758–770
25. Matsumura, S., Saitou, K., Miyaki, T., Yoneda, T., Mizushige, T., Eguchi, A., Shibakusa, T., Manabe, Y., Tsuzuki, S., Inoue, K., and Fushiki, T. (2008) Mercaptoacetate inhibition of fatty acid $\beta$-oxidation attenuates the oral acceptance of fat in BALB/c mice. *Am. J. Physiol. Regul. Integr. Comp. Physiol.* **295,** R82–R91
26. Ohkawa, H., Ohishi, N., and Yagi, K. (1979) Assay for lipid peroxides in animal tissues by thiobarbituric acid reaction. *Anal. Biochem.* **95,** 351–358
27. Suzuki, J., Shen, W. J., Nelson, B. D., Selwood, S. P., Murphy, G. M., Jr., Kanehara, H., Takahashi, S., Oida, K., Miyamori, I., and Kraemer, F. B. (2002) Cardiac gene expression profile and lipid accumulation in response to starvation. *Am. J. Physiol. Endocrinol. Metab.* **283,** E94–E102
28. Granneman, J. G., Moore, H. P., Mottillo, E. P., and Zhu, Z. (2009) Functional interactions between Mldp (LSDP5) and Abhd5 in the control of intracellular lipid accumulation. *J. Biol. Chem.* **284,** 3049–3057
29. Masuda, Y., Itabe, H., Odaki, M., Hama, K., Fujimoto, Y., Mori, M., Sasabe, N., Aoki, J., Arai, H., and Takano, T. (2006) ADRP/adipophilin is degraded through the proteasome-dependent pathway during regression of lipid-storing cells. *J. Lipid Res.* **47,** 87–98
30. Xu, G., Sztalryd, C., Lu, X., Tansey, J. T., Gan, J., Dorward, H., Kimmel, A. R., and Londos, C. (2005) Post-translational regulation of adipose differentiation-related protein by the ubiquitin/proteasome pathway. *J. Biol. Chem.* **280,** 42841–42847
31. Jenkins, C. M., Mancuso, D. J., Yan, W., Sims, H. F., Gibson, B., and Gross, R. W. (2004) Identification, cloning, expression, and purification of three novel human calcium-independent phospholipase A2 family members possessing triacylglycerol lipase and acylglycerol transacylase activities. *J. Biol. Chem.* **279,** 48968–48975
32. Luiken, J. J., van Nieuwenhoven, F. A., America, G., van der Vusse, G. J., and Glatz, J. F. (1997) Uptake and metabolism of palmitate by isolated cardiac myocytes from adult rats. Involvement of sarcolemmal proteins. *J. Lipid Res.* **38,** 745–758
33. Griesel, B. A., Weems, J., Russell, R. A., Abel, E. D., Humphries, K., and Olson, A. L. (2010) Acute inhibition of fatty acid import inhibits GLUT4 transcription in adipose tissue, but not skeletal or cardiac muscle tissue, partly through liver X receptor (LXR) signaling. *Diabetes* **59,** 800–807
34. Balaban, R. S., Nemoto, S., and Finkel, T. (2005) Mitochondria, oxidants, and aging. *Cell* **120,** 483–495
35. Xu, Q., Dalic, A., Fang, L., Kiriazis, H., Ritchie, R. H., Sim, K., Gao, X. M., Drummond, G., Sarwar, M., Zhang, Y. Y., Dart, A. M., and Du, X. J. (2011) Myocardial oxidative stress contributes to transgenic $\beta_2$-adrenoceptor activation-induced cardiomyopathy and heart failure. *Br. J. Pharmacol.* **162,** 1012–1028
36. Granneman, J. G., Moore, H. P., Mottillo, E. P., Zhu, Z., and Zhou, L. (2011) Interactions of perilipin-5 (Plin5) with adipose triglyceride lipase. *J. Biol. Chem.* **286,** 5126–5135
37. Wang, H., Bell, M., Sreenevasan, U., Hu, H., Liu, J., Dalen, K., Londos, C., Yamaguchi, T., Rizzo, M. A., Coleman, R., Gong, D., Brasaemle, D., and Sztalryd, C. (2011) Unique regulation of adipose triglyceride lipase (ATGL) by perilipin 5, a lipid droplet-associated protein. *J. Biol. Chem.* **286,** 15707–15715
38. Wang, H., Hu, L., Dalen, K., Dorward, H., Marcinkiewicz, A., Russell, D., Gong, D., Londos, C., Yamaguchi, T., Holm, C., Rizzo, M. A., Brasaemle, D., and Sztalryd, C. (2009) Activation of hormone-sensitive lipase requires two steps, protein phosphorylation and binding, to the PAT-1 domain of lipid droplet coat proteins. *J. Biol. Chem.* **284,** 32116–32125
39. Wang, Z., Heshka, S., Gallagher, D., Boozer, C. N., Kotler, D. P., and Heymsfield, S. B. (2000) Resting energy expenditure-fat-free mass relationship. New insights provided by body composition modeling. *Am. J. Physiol. Endocrinol. Metab.* **279,** E539–E545
40. Gotto, A. M., Jr., Pownall, H. J., and Havel, R. J. (1986) Introduction to the plasma lipoproteins. *Methods Enzymol.* **128,** 3–41
41. Bartholomew, S. R., Bell, E. H., Summerfield, T., Newman, L. C., Miller, E. L., Patterson, B., Niday, Z. P., Ackerman, W. E., 4th, and Tansey, J. T. (2012) Distinct cellular pools of perilipin 5 point to roles in lipid trafficking. *Biochim. Biophys. Acta* **1821,** 268–278
42. Wang, H., Sreenevasan, U., Hu, H., Saladino, A., Polster, B. M., Lund, L. M., Gong, D. W., Stanley, W. C., and Sztalryd, C. (2011) Perilipin 5, a lipid droplet-associated protein, provides physical and metabolic linkage to mitochondria. *J. Lipid Res.* **52,** 2159–2168
43. Stein, O., and Stein, Y. (1968) Structures and physiological roles of 13 integral lipids of bovine heart cytochrome *c* oxidase. *J. Cell Biol.* **36,** 63–77
44. Shinzawa-Itoh, K., Aoyama, H., Muramoto, K., Terada, H., Kurauchi, T., Tadehara, Y., Yamasaki, A., Sugimura, T., Kurono, S., Tsujimoto, K., Mizushima, T., Yamashita, E., Tsukihara, T., and Yoshikawa, S. (2007) Structures and physiological roles of 13 integral lipids of bovine heart cytochrome *c* oxidase. *EMBO J.* **26,** 1713–1725
45. Seddon, M., Looi, Y. H., and Shah, A. M. (2007) Oxidative stress and redox signaling in cardiac hypertrophy and heart failure. *Heart* **93,** 903–907

Clin Pediatr Endocrinol 2013; 22(4), 53–64


## Original Article

# Abnormal Adipose Tissue Distribution with Unfavorable Metabolic Profile in Five Children Following Hematopoietic Stem Cell Transplantation: A New Etiology for Acquired Partial Lipodystrophy

Masanori Adachi[1], Yumi Asakura[1], Koji Muroya[1], Hiroaki Goto[2], and Hisato Kigasawa[2]

[1]*Department of Endocrinology and Metabolism, Kanagawa Children's Medical Center, Yokohama, Japan*

[2]*Department of Hematology and Regenerative Medicine, Kanagawa Children's Medical Center, Yokohama, Japan*

**Abstract.** We report five consecutive patients who underwent hematopoietic stem cell transplantation (HSCT) to treat leukemia or neuroblastoma early in their lives and later manifested abnormal patterns of adipose tissue distribution. Lipoatrophy was remarkable in the gluteal regions and extremities, whereas subcutaneous fat was preserved in the cheeks, neck, and abdomen. In addition, visceral fat deposition, fatty changes in the liver, and metabolic derangements such as insulin resistance and hypertriglyceridemia were evident. These features resemble Dunnigan-type familial partial lipodystrophy, which is a rare condition caused by *LMNA* gene mutation. These patients shared a common medical history involving HSCT, including conditioning with total body irradiation (TBI). They also received intensive chemotherapy because of multiple metastases (n = 3), relapse (n = 3), and repetitive HSCT (n = 3). We propose HSCT as a new etiology for acquired partial lipodystrophy and recommend that patients who undergo HSCT with TBI and intensive chemotherapy early in their lives must receive careful observation for the possible development of lipodystrophy and metabolic complications.

**Key words:** chemotherapy, dyslipidemia, hypertriglyceridemia, insulin resistance, total body irradiation

## Introduction

Partial lipodystrophy refers to a pathological and unique fat distribution, characterized by lipoatrophy (loss of adipose tissue) and lipohypertrophy (abnormal fat accumulation) (1, 2). Metabolic complications such as insulin resistance, diabetes, hypertriglyceridemia, and fatty changes in the liver are additional hallmarks of partial lipodystrophy (1–4).

Familial partial lipodystrophy (FPLD) arises from genetic mutations, including mutations in the *LMNA* (5–7), *PPARγ* (8–10), *AKT2* (11) and *CIDEC* (12) genes. Specifically, FPLD caused by a *LMNA* mutation is referred to as Dunnigan-type FPLD, or FPLD2, and is characterized by lipoatrophy in the extremities and buttocks combined with fat accumulation in the face, neck

Received: May 31, 2013
Accepted: July 1, 2013
Corresponding author: Dr. Masanori Adachi, Department of Endocrinology and Metabolism, Kanagawa Children's Medical Center, 2-138-4 Mutsukawa, Minami-ku, Yokohama 232-8555, Japan
E-mail: madachi@mars.sannet.ne.jp

and intra-abdominal areas. Among the acquired forms of partial lipodystrophy, the most prevalent one is highly active antiretroviral therapy (HAART)-associated lipodystrophy syndrome found in HIV-infected individuals (13, 14). Acquired partial lipodystrophy can also develop following viral infection, autoimmune disease or membranous proliferative glomerulonephritis (1).

We treated 5 consecutive patients who had previously undergone hematopoietic stem cell transplantation (HSCT) to treat malignancies at a younger age. These patients, later in their lives, manifested aberrant fat distribution patterns similar to those occurring in patients with FPLD2, as well as severe metabolic abnormalities.

## Case Series

All the study procedures, including the control subjects in body composition analysis, were reviewed and approved by the ethics committee of Kanagawa Children's Medical Center. Patients 2, 3, 4, and 5 and the mother of patient 1 provided written informed consent for publication of their facial photographs.

### Patient 1, female, acute myeloid leukemia (AML)

As a result of an evaluation of walking difficulties and repetitive, febrile episodes, a 1-yr-old girl was diagnosed with AML, classified as M4, with multiple extra-marrow involvements, including the central nervous system. Following successful induction chemotherapy, bone marrow transplantations (BMTs) from her mother were attempted twice, but were rejected. A third allogeneic BMT, with conditioning that included total body irradiation (TBI) of 10 Gy, was successful and resulted in long-term remission. However, the patient developed chemotherapy-related leukoencephalopathy, and suffered from intractable epilepsy. To suppress extensive, chronic, graft-versus-host disease (GVHD) (15), she had received steroid therapy for 3 yr (Table 1).

At 17 yr of age, the patient underwent her first endocrinological evaluation (Table 2) because she was short [130.3 cm, –5.3 SD for Japanese standards (16)] and prepubertal. Subcutaneous fat was rather abundant in her cheeks and neck, which resulted in a moon-face appearance (Fig. 1a). In addition, the patient exhibited remarkable abdominal distension, with an abdominal circumference of 69 cm at the navel level. However, both her extremities and buttocks showed marked reductions in subcutaneous fat tissue (Fig. 1b).

An oral glucose tolerance test (OGTT) showed a diabetic blood glucose pattern with tremendous hyperinsulinism (Fig. 2). Mildly elevated alanine aminotransferase (ALT) (56 IU/L) and γ glutamyl transpeptidase (γ GTP) (387 IU/L) levels were found, and fatty changes in the liver were suspected based on abdominal ultrasonography (US). Dyslipidemia was also evident, with fasting triglyceride (TG) levels of 675 mg/dL, high-density lipoprotein cholesterol (HDL-C) of 39 mg/dL and low-density lipoprotein cholesterol (LDL-C) of 168 mg/dL (Table 3).

A magnetic resonance imaging scan revealed a small pituitary gland, and the patient was found to have GH deficiency, subclinical hypothyroidism (TSH, 5.45 μIU/L; free T4, 0.93 ng/dL), and primary ovarian insufficiency (FSH, 60.9 IU/L) (Tables 1 and 2).

### Patient 2, female, AML

An 8-yr-old girl was diagnosed with AML (M2) through an evaluation for petechiae and epistaxis. Six mo after the first remission was achieved by chemotherapy, a marrow relapse was found. A BMT from a human leukocyte antigen (HLA)-identical donor was conducted, following conditioning that included TBI of 12 Gy. Chronic GVHD with pneumonitis, joint contractures and liver dysfunction required immunosuppressive treatment lasting more than a decade. She also suffered from right-sided femoral neck necrosis (with an onset at age 12), transient aplastic anemia following a parvovirus infection (at age 13) and multiple hepatic angiomas (at age 17).

**Table 1** Treatment summaries for the original malignancies in the 5 patients

| Pt (sex) | Primary disease (onset) | Treatment | | | Chronic graft-versus-host disease classification and treatment[@] | Treatment-related complications |
|---|---|---|---|---|---|---|
| | | Chemo-therapy* | Radiation (site) | Transplantation (conditioning[#]) | | |
| 1 (F) | AML (1 yr) | VP-16, Ara-C, MIT, THP-ADR, ACR, VCR, MTX (it), HC (it) | ND | Failed 2 consecutive allogeneic BMTs (BSF, VP-16, L-PAM) Successful third allogeneic BMT (TBI 10 Gy, ATG, TT) | Extensive (skin, liver) CsA (for 1.5 yr), PSL (for 3 yr) | GH deficiency (untreated), hypothyroidism (treated from age 17 yr), leukoencephalopathy, epilepsy, primary hypogonadism (treated from age 17 yr) |
| 2 (F) | AML (8 yr) | VP-16, Ara-C, MIT, IDR, MTX (it), HC (it) | ND | Unrelated BMT following marrow relapse (TBI 12 Gy, BSF, L-PAM) | Extensive (lung, joint, liver) PSL (for 12 yr), FK-506 (for 12 yr) | Femoral neck necrosis, aplastic anemia, hepatic angioma, hypothyroidism (treated from age 15 yr), primary hypogonadism (treated from age 19 yr) |
| 3 (M) | ALL (0 yr) | VCR, THP-ADR, L-ASP, MTX, CPM, Ara-C, 6-MP, PSL, DEX | 18 Gy (cranial) | 2 consecutive allogeneic BMTs following marrow relapse [ 1) TBI 12 Gy, VP-16, Ara-C, CPM 2) BSF, VP-16, Ara-C,CPM] | Extensive (skin, joint) CsA (for 4 yr), AZA (for 9 yr), PSL (for 12 yr), MTX (for 1 yr) | GH treatment (from age 11 to 17 yr), chronic thyroiditis (no treatment) |
| 4 (M) | NB (1 yr) | CPM, VP-16, THP-ADR, CDDP, CBDCA | 23.4 Gy (cranial), 18 Gy (right orbit) | Scheduled PBSCT (TBI 12 Gy, CBDCA, VP-16, L-PAM) | None | Hypothyroidism (treated from age 4 yr), empty sella, GH deficiency (treated from age 14 to 20 yr), hypogonadism (treated from age 18 yr) |
| 5 (F) | NB (1 yr) | CPM, VP-16, THP-ADR, CDDP, DTIC, IFM | 19.8 Gy (epigastrium), 30 Gy (right iliac) | 2 consecutive autologous BMTs [1) CBDCA, THP-ADR, L-PAM, 2) CBDCA, VP-16, THP-ADR, CPM], allogeneic BMT following regional and marrow relapse (TBI 12 Gy, TT, VP-16) | Extensive (liver, intestine) FK-506 (for 3 yr), PSL (for 3 yr) | GH deficiency (treated from age 11 to 17 yr), primary hypogonadism (treated from age 15 yr), high-frequency deafness, cataract |

F, female; M, male; ND, not done; it, intrathecal injection; BMT, bone marrow transplantation; PBSCT, peripheral blood stem cell transplantation; rt, right. *Abbreviations for agents: VP-16, etoposide; Ara-C, cytarabine; MIT, mitoxantrone hydrochloride; THP-ADR, tetrahydropyranyladriamycin; ACR, aclarubicin hydrochloride; VCR, vincristine sulfate; MTX, methotrexate; HC, hydrocortisone; IDR, idarubicin hydrochloride; L-ASP, L-asparaginase; CPM, cyclophosphamide; 6-MP, 6-mercaptopurine; PSL, prednisolone; DEX, dexamethasone; CDDP, cisplatin; CBDCA, carboplatin; DTIC, dacarbazine; IFM, ifosfamide. [#]BSF, busulfan; L-PAM, melphalan; ATG, antithymocyte globulin; TT, Thio-TEPA; [@]CsA, cyclosporin A; FK-506, tacrolimus; AZA, azathioprine.


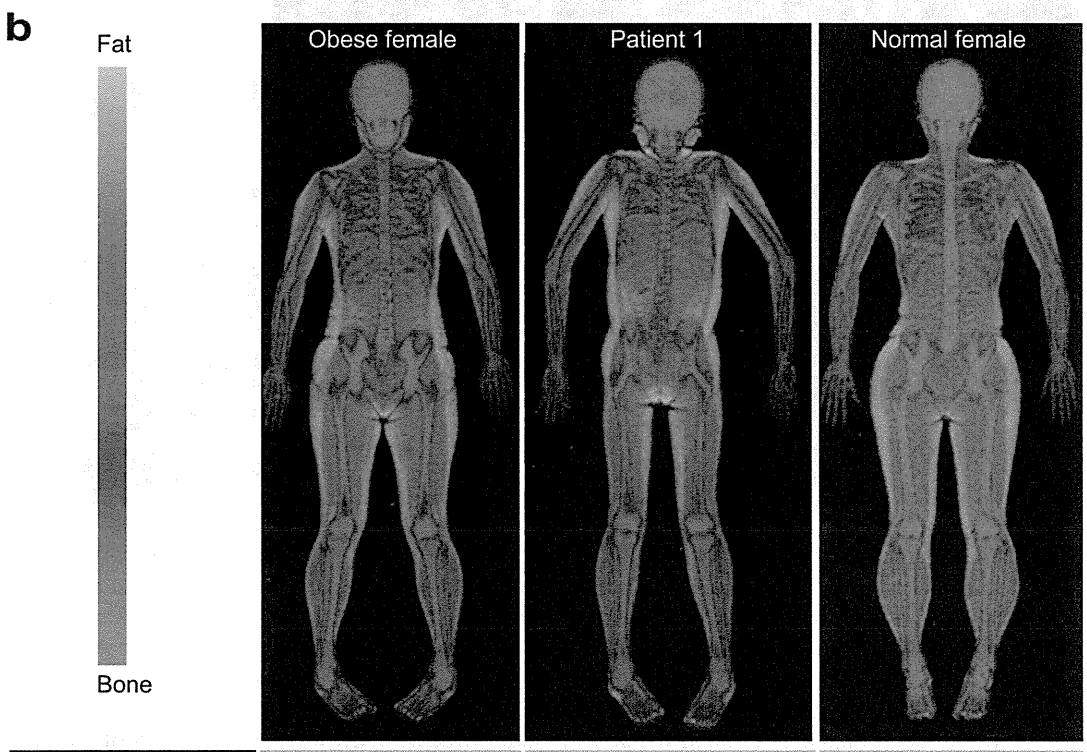


| | | Obese female | Patient 1 | Normal female |
|---|---|---|---|---|
| % fat | upper extremities | 54.7 | 40.5 | 28.1 |
| | trunk | 38.5 | 28.4 | 18.1 |
| | lower extremities | 35.0 | 35.5 | 30.6 |
| | total body | 37.2 | 31.2 | 23.7 |

When the patient was 15 yr old, abnormal fat distribution was ascertained by whole body computed tomography (CT) (Fig. 1c). An OGTT showed a normal blood glucose response but with hyperinsulinism (Fig. 2). Dyslipidemia and fatty changes in the liver were also noticed. An endocrinological evaluation revealed mild hypothyroidism (TSH, 9.28 μIU/mL; free T4, 0.89 ng/dL) with primary hypogonadism (FSH, 217.9 IU/L; E2, 5.6 pg/mL).

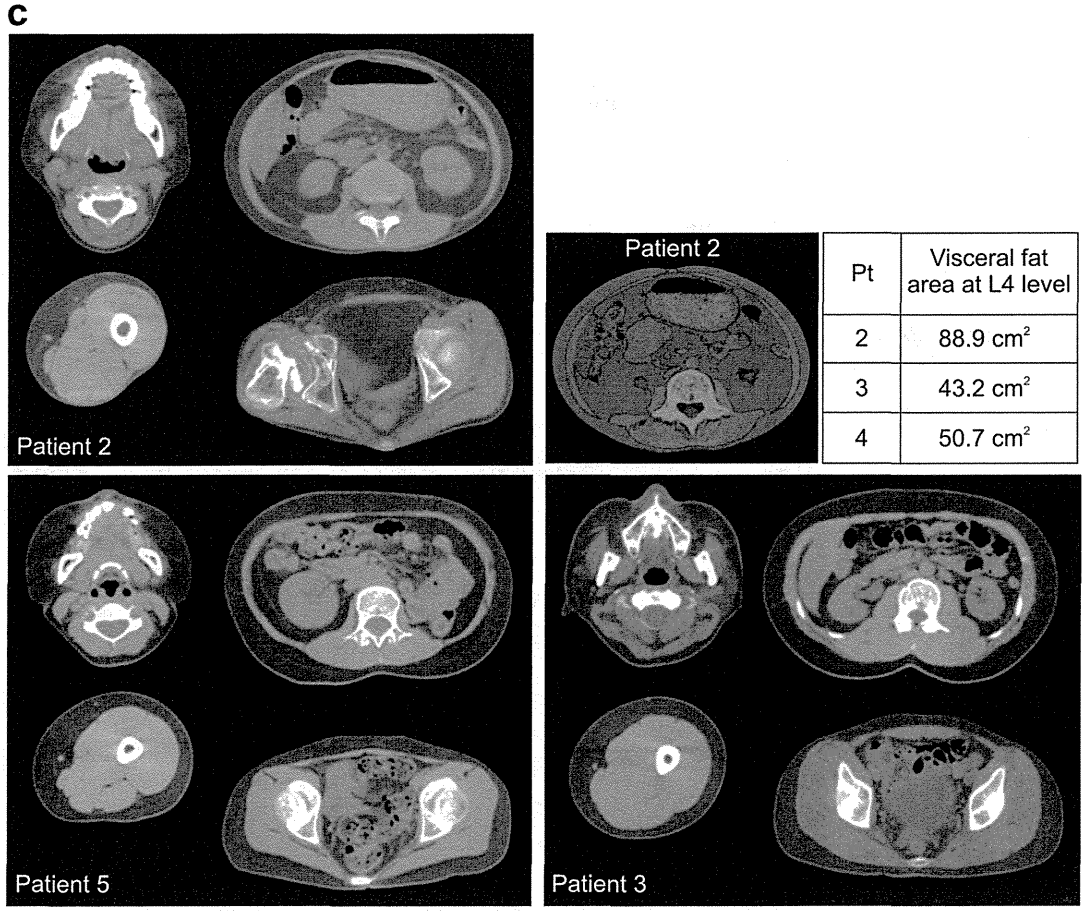


**Fig. 1.** Abnormal fat distribution observed in the patients. a) Facial photos of the patients. Note that the increased subcutaneous fat tissue in the cheeks gives the impression of a moon-face. b) Dual-energy X-ray absorptiometry image of patient 1 (middle) at age 18 yr. Compared with a 25-yr-old obese woman (left), lipoatrophy in the hips and legs and lipohypertrophy in the neck are evident. For comparison, an image of a nonobese, healthy, 29-yr-old woman is also shown (right). Fat content values of various portions of the body are provided under the images. c) Typical whole-body computed tomography scans of patient 2 at age 18 yr, patient 3 at age 19 yr, and patient 5 at age 18 yr. Increased subcutaneous cheek and visceral fat is evident, whereas loss of subcutaneous fat is remarkable in both the buttocks and thighs. In the inset table, the visceral fat area at the $4^{th}$ lumbar spine level in each patient is provided, along with the image obtained from patient 2.

### Patient 3, male, acute lymphoid leukemia (ALL)

This patient was diagnosed with unclassified ALL at 11 mo of age as a result of an evaluation of petechiae. His first remission was achieved by chemotherapy and 18 Gy cranial radiation. A year later, marrow relapse was found. Following chemotherapy, two consecutive allogeneic BMTs were conducted, with 12 Gy TBI conditioning being provided before the first round of BMT (Table 1).

Chronic GVHD, with major symptoms of joint contractures and scleroderma, was treated with immunosuppressants. In accordance with

**Table 2** Current status and information relevant to the etiology of lipodystrophy in the 5 patients

| Patient | Current status | | | At diagnosis of lipodystrophy | | | | Estimated onset of lipodystrophy* (yr) | *LMNA* mutation |
|---|---|---|---|---|---|---|---|---|---|
| | Age (yr) | BMI (kg/m$^2$) | Typical fat distribution$^{\$}$ | Age (yr) | GH status | Thyroid status | Gonadal status | | |
| 1 | 18 | 17.7 | + | 17 | Deficient | Hypothyroid | Hypogonadal | 11 | Absent |
| 2 | 21 | 12.2 | + | 15 | Sufficient | Hypothyroid | Hypogonadal | 13 | Absent |
| 3 | 23 | 16.5 | + | 19 | Sufficient$^{\#}$ | Euthyroid | Eugonadal | 12 | Absent |
| 4 | 21 | 18.3 | + | 19 | Replacement therapy for 5 yr | Replacement therapy for 15 yr | Replacement therapy for 1 yr | 15 | ND |
| 5 | 22 | 14.1 | + | 17 | Replacement therapy for 5 yr | Euthyroid | Replacement therapy for 2 yr | 14 | Absent |

+, present; BMI, body mass index; ND, not determined. $^{\$}$Typical fat distribution denotes lipoatrophy in the gluteal region and extremities coupled with preserved, or even prominent, subcutaneous fat in the cheeks, neck and abdomen. *Onset of lipodystrophy as deduced from the emergence of an elevated triglyceride level. (For details, refer to the Methods section.) $^{\#}$GH treatment was conducted from 11 to 17 yr of age despite normal GH secretion.

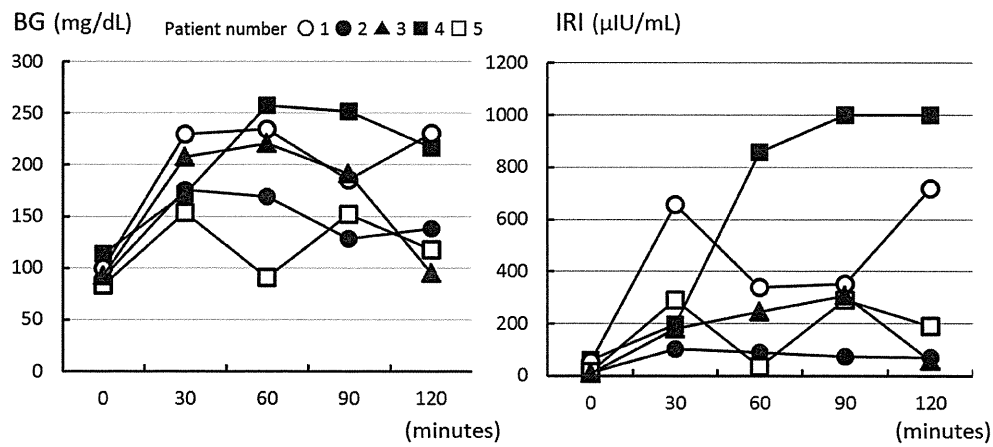


**Fig. 2.** Results of a 75-g oral glucose tolerance test in the 5 patients. Left panel, blood glucose (BG) response; right panel, insulin response. In the criteria developed by the Japanese Diabetes Society, the diabetic pattern is defined as the fasting blood glucose being higher than 126 mg/dL or the blood glucose level at 120 min being higher than 200 mg/dL. The normal pattern is defined as a fasting blood glucose less than 110 mg/dL and a blood glucose level of less than 140 mg/dL at 120 min.

his wishes, GH treatment was conducted for 6 yr beginning at age 11 despite normal GH secretion. Nevertheless, his final height was 142.4 cm (–4.9 SD).

Thinning of the extremities, due to subcutaneous fat loss, and a moon-face appearance were noticed when the patient was 13 yr old. A whole body CT scan taken at age 19 revealed fatty changes in the liver and an abnormal pattern of subcutaneous fat distribution (Fig. 1c). Dyslipidemia and hyperinsulinism were also evident.

**Table 3** Summary of the metabolic profile of the 5 patients

| Patient | Fatty liver | | Lipid | | | | | Adipokines | | Diabetes | | | | |
|---|---|---|---|---|---|---|---|---|---|---|---|---|---|---|
| | US/CT | ALT (IU/L) | TC (mg/dL) | LDL-C (mg/dL) | TG (mg/dL) | HDL-C (mg/dL) | Treatment | Leptin* (ng/mL) | Adiponectin# (μg/mL) | BG response in OGTT (age) | Insulinogenic index | HOMA-R | HbA1c | Treatment |
| 1 | + | 56 | 322 | 168 | 675 | 39 | none | 18.7 | 1.6 | DM pattern (17 y) | 4.63 | 13.3 | 6.1% | none |
| 2 | + | 102 | 375 | 203 | 965 | 50 | none | 9.5 | 6.8 | normal (18 y) | 1.06 | 2.92 | 5.4% | none |
| 3 | + | 85 | 284 | 179 | 901 | 44 | fenofibrate | 10.7 | 8.5 | normal (13 y) | 1.04 | 2.11 | 5.3% | none |
| | | | | | | | | | | normal (23 y) | 1.47 | 1.98 | 5.1% | |
| 4 | + | 137 | 314 | 176 | 1,073 | 44 | none | 17.9 | 1.7 | DM pattern (19 y) | 2.34 | 17.0 | 5.7% | none |
| 5 | + | 250 | 203 | 124 | 402 | 35 | none | 11.9 | 3.8 | normal (21 y) | 3.89 | 3.15 | 5.2% | none |

+, present; US, ultrasound; CT, computed tomography; ALT, alanine aminotransferase; TC, total cholesterol; LDL-C, LDL-cholesterol; TG, triglyceride; HDL-C, HDL-cholesterol; HOMA-R, homeostasis model assessment ratio; BG, blood glucose; DM, diabetes mellitus; ND, not determined. Each value is the highest one ever determined, except for HDL-C where the lowest value is presented. *Leptin levels in healthy Japanese adolescents were reported to be 1.65 ± 0.78 ng/mL in males and 6.03 ± 3.69 ng/mL in females (35). #Adiponectin levels in healthy young Japanese women were reported to be 6.2–10.0 μg/mL (36). In addition, adiponectin level lower than 6.65 μg/mL was suggested as a diagnostic marker of metabolic syndrome in Japanese children (37).

### Patient 4, male, neuroblastoma

A 1-yr-old boy developed exophthalmos and neuroblastoma, originating from the left adrenal, with multiple bone and marrow metastases (stage $IV_A$). Following total resection of the primary lesion, complete remission was obtained by chemotherapy and radiation (whole skull, 23.4 Gy; right orbit, 18 Gy). Eight months after diagnosis, peripheral blood stemcell transplantation (PBSCT) was carried out, with conditioning that included 12 Gy TBI.

Since age 4, the patient has been receiving L-thyroxine because of primary hypothyroidism (TSH, 22.0 μIU/mL; free T4, 0.78 ng/dL). At age 14, an evaluation for growth failure revealed severe atrophy of the pituitary gland. At that time, abdominal US demonstrated fatty changes in his liver. After a diagnosis of complete GH deficiency, GH treatment was started. At age 18, testosterone administration was introduced due to primary hypogonadism (LH, 7.6 IU/L; FSH, 26.6 IU/L; testosterone, 51 ng/dL).

At 19 yr of age, abnormal liver function tests, dyslipidemia and a moon-face appearance prompted a metabolic reevaluation. Although the degree of aberrant fat distribution was modest compared with other patients, a CT scan demonstrated increased visceral fat with a markedly fatty liver. A diabetic pattern of blood glucose response was observed in an OGTT, as well as pronounced hyperinsulinism.

### Patient 5, female, neuroblastoma

A neuroblastoma, with multiple bone metastases (stage $IV_A$), was diagnosed in a 1-yr-old female during the evaluation of an abdominal mass. Following total removal of the primary tumor and chemotherapy, two consecutive autologous BMTs, without TBI, were performed 3-mo apart. A regional relapse in the right iliac bone, as well as marrow relapse, was found one year later. The patient was treated with an allogeneic BMT, the donor being her 2-locus mismatched sister, following 12 Gy TBI conditioning. Thereafter, complete remission was obtained, and immunosuppressants were withdrawn at age 8.

Partial GH deficiency was diagnosed at age 12, and GH treatment was conducted for 5 yr. The patient also exhibited primary hypogonadism, high-frequency deafness and the presence of cataracts. At around age 17, fatty

changes in the liver and hypertriglyceridemia developed, followed by a mild, abnormal pattern of subcutaneous fat distribution. An OGTT showed normal blood glucose responses, but with hyperinsulinism.

### Methods and Results

Body composition analysis with dual-energy X-ray absorptiometry was performed in patient 1 using a Discovery® A Densitometer (Hologic, Inc., Bedford, MA, USA) in fan beam analysis mode and software version 13.3.0.1 (Fig. 1b). To illustrate fat distribution abnormality clearly, a 25-yr-old obese woman and a 29-yr-old healthy nonobese woman served as controls. In the former, this analysis was carried out as one of the routine medical evaluations for obesity.

Visceral fat area at the $4^{th}$ lumbar spine level was determined with FatVizCalc® (LISIT Co., Ltd., Tokyo, Japan) using the CT images of each patient (Fig. 1c).

Written informed consent for *LMNA* gene analysis was obtained from patients 2, 3 and 5 and from the mother of patient 1. Patient-specific gDNA was extracted from a nail specimen, and the common mutations in exons 8 and 11 of the *LMNA* gene, associated with FPLD2, were studied, as previously described (17). The mutation was absent in these patients (Table 2).

The onset of lipodystrophy is difficult to ascertain because the attending hematologists, as well as the patients themselves, are unaware of fat distribution abnormalities. Because serum triglyceride levels were routinely measured in the patients, we deduced the onset of lipodystrophy based on the timing of emergence of an elevated triglyceride level. As listed in Table 2, lipodystrophy seemed to develop about a decade after HSCT.

## Discussion

All the described patients demonstrated a characteristic adipose tissue distribution pattern. Lipoatrophy was remarkable in the gluteal region and extremities, whereas subcutaneous fat was preserved, or even prominent, in the cheeks, neck and abdomen. Visceral fat deposition, as well as fatty changes in the livers of these patients, was also evident. This particular distribution pattern resembles that seen in FPLD2, which is caused by a *LMNA* gene mutation (1, 2, 5–7). Patients with this rare entity, which has an estimated prevalence of 1 in 15 million individuals (1), manifest a peculiar lipodystrophy after adolescence. In addition, metabolic complications, including insulin resistance, diabetes, hypertriglyceridemia, low HDL cholesterol levels and fatty liver, are prevalent in FPLD2 patients (3, 4). Female patients also have an increased risk for developing polycystic ovary syndrome and infertility (18). Compared with generalized lipodystrophy and other types of partial lipodystrophy, leptin and adiponectin levels in FPLD2 are only modestly decreased (19). However, FPLD2 is unlikely the cause of lipodystrophy in these patients, considering its low prevalence and the absence of *LMNA* gene mutations in the 4 patients tested.

Our patients and those with FPLD2 share similarities in fat distribution patterns and in metabolic derangements. Pronounced hypertriglyceridemia, coupled with decreased HDL cholesterol levels, was present in the 5 patients; elevated LDL cholesterol, defined as levels above 150 mg/dL, was present in 4 patients. The patients had high homeostasis model assessment ratios (HOMA-Rs), indicating insulin resistance, although acanthosis nigricans was not observed in any patients. Two patients had OGTTs that categorized them into the diabetic pattern according to the criteria developed by the Japanese Diabetes Society (see Fig. 2 legend). The patients with the diabetic pattern were found to have pronounced hyperinsulinemia with a peak insulin level exceeding 700 μIU/mL. In the present cases, the levels of leptin and adiponectin were modestly decreased.

The patients described in this report shared a common medical history that included HSCT

and conditioning with 10–12 Gy TBI. All of them also received intensive chemotherapy because of the severe nature of their diseases, including widespread metastases (patients 1, 4 and 5) and early relapses (patients 2, 3 and 4), and/or repetitive HSCT (patients 1, 3 and 5). Major surgery, however, was only conducted on those with neuroblastomas. Cranial radiation was performed on only 3 patients.

Based on the above observations, we propose HSCT as a new etiology for acquired partial lipodystrophy. Partial lipodystrophy seems to develop following HSCT, including TBI, especially in conjunction with intensive chemotherapy. This outcome appears to occur irrespective of other interventions such as surgery and cranial radiation. Younger age at the time of HSCT may be of significance, considering that 4 patients received transplants during infancy.

We speculate that TBI and/or intensive chemotherapy may damage the function of adipocytes in the subcutaneous fat, thereby limiting their lipid-storage capacity. This may lead to ectopic deposition of fat in visceral adipose tissue, muscle and liver. This hypothesis is reasonable because adipose tissue fibrosis, and the resultant ectopic lipid accumulation, has been demonstrated in obese individuals (20). Although the mechanism for the characteristic pattern of lipodystrophy is unclear, it may reflect the site-specific adipose tissue functions. In a subset of partial lipodystrophy accompanying glomerulonephritis, differential expression of complementary D by various adipose tissues is considered to cause the different degrees of lipodystrophy among the body (21).

It is essential to consider other potential factors that may be relevant to the development of lipodystrophy. Rooney and Ryan (22) reported a female patient who underwent allogeneic HSCT for relapsed ALL and developed partial lipodystrophy, with overt diabetes, 9 yr later. This patient had GVHD-associated scleroderma, and these authors speculated that there was a causative relationship between partial lipodystrophy and scleroderma. This hypothesis is very intriguing considering that decreased adiponectin levels have been described in systemic sclerodermas with autoimmune origins (23, 24). However, the severity of the GVHD varied among our patients, and scleroderma was present only in patient 3. GVHD was entirely absent in patient 4, who underwent autologous HSCT. Therefore, GVHD and GVHD-related scleroderma may not be a prerequisite but may be a predisposing factor for the development of partial lipodystrophy.

Another factor that should be considered is endocrinopathy. Four patients had endocrinological complications such as GHD, hypothyroidism and hypogonadism (Table 2). Although some of these endocrinopathies had been treated at the time of the investigation, hormone deficiency must be present for a significant period before the initiation of hormonal therapy. At present, endocrinopathy, *per se*, is not regarded as a definite cause of lipodystrophy (1, 2). However, endocrinological complications may be likely to modify the development and/or progress of lipodystrophy, considering that each hormone has its own receptor in the adipose tissue (25, 26), and the relationship between hormonal deficiency and metabolic complications is well-known (27, 28).

A causative relationship between HSCT and lipodystrophy may be disputed based on the absence of reports other than that of Rooney and Ryan (22). However, in accordance with our proposal, a high incidence of fatty liver was also reported in individuals who have undergone HSCT (29). In addition, radiation therapy, including TBI, is an established risk factor for developing metabolic syndrome (30, 31). Moreover, impaired glucose tolerance and dyslipidemia have been described as late complications following HSCT (32–34). We infer that a substantial number of partial lipodystrophy patients may have gone undiagnosed because careful observations are necessary to detect abnormal fat distribution

and because lipodystrophy is not a well-known condition, especially among pediatricians.

To clarify the incidence of HSCT-related lipodystrophy, as well as the contributions of GVHD, GVHD-scleroderma and endocrinopathies, further studies are clearly needed. Lipodystrophy appears to develop more than a decade after HSCT. In addition, the progress of lipodystrophy may be slow, considering that the OGTT results did not differ over a 10-yr interval in patient 3 (Table 3). Thus, prospective studies with long observation periods may be needed to clarify the reality of this potentially life-threatening complication in childhood cancer survivors.

## Conclusion

Five pediatric patients manifesting aberrant fat distribution patterns similar to those observed in FPLD2 patients and severe metabolic abnormalities were described. Patients undergoing HSCT, especially when performed early in their lives and in conjunction with TBI and intensive chemotherapy, warrant careful observation for the potential development of partial lipodystrophy.

## Acknowledgments

We thank Dr. Kumiko Nozawa and Dr. Noriko Aida, Department of Radiology, Kanagawa Children's Medical Center, for their valuable assistance in preparing the CT and DEXA images.

## References

1. Fiorenza CG, Chou SH, Mantzoros CS. Lipodystrophy: pathophysiology and advances in treatment. Nat Rev Endocrinol 2011;7: 137–50. [Medline]
2. Garg A. Acquired and inherited lipodystrophies. N Engl J Med 2004;350: 1220–34. [Medline]
3. Schmidt HH, Genschel J, Baier P, Schmidt M, Ockenga J, Tietge UJ, *et al.* Dyslipidemia in familial partial lipodystrophy caused by an R482W mutation in the LMNA gene. J Clin Endocrinol Metab 2001;86: 2289–95. [Medline]
4. Lüdtke A, Genschel J, Brabant G, Bauditz J, Taupitz M, Koch M, *et al.* Hepatic steatosis in Dunnigan-type familial partial lipodystrophy. Am J Gastroenterol 2005;100: 2218–24. [Medline]
5. Cao H, Hegele RA. Nuclear lamin A/C R482Q mutation in Canadian kindreds with Dunnigan-type familial partial lipodystrophy. Hum Mol Genet 2000;9: 109–12. [Medline]
6. Speckman RA, Garg A, Du F, Bennett L, Veile R, Arioglu E, *et al.* Mutational and haplotype analyses of families with familial partial lipodystrophy (Dunnigan variety) reveal recurrent missense mutations in the globular C-terminal domain of lamin A/C. Am J Hum Genet 2000;66: 1192–8. [Medline]
7. Shackleton S, Lloyd DJ, Jackson SN, Evans R, Niermeijer MF, Singh BM, *et al.* LMNA, encoding lamin A/C, is mutated in partial lipodystrophy. Nat Genet 2000;24: 153–6. [Medline]
8. Barroso I, Gurnell M, Crowley VE, Agostini M, Schwabe JW, Soos MA, *et al.* Dominant negative mutations in human PPARgamma associated with severe insulin resistance, diabetes mellitus and hypertension. Nature 1999;402: 880–3. [Medline]
9. Hegele RA, Cao H, Frankowski C, Mathews ST, Leff T. PPARG F388L, a transactivation-deficient mutant, in familial partial lipodystrophy. Diabetes 2002;51: 3586–90. [Medline]
10. Agarwal AK, Garg A. A novel heterozygous mutation in peroxisome proliferator-activated receptor-gamma gene in a patient with familial partial lipodystrophy. J Clin Endocrinol Metab 2002;87: 408–11. [Medline]
11. George S, Rochford JJ, Wolfrum C, Gray SL, Schinner S, Wilson JC, *et al.* A family with severe insulin resistance and diabetes due to a mutation in AKT2. Science 2004;304: 1325–8. [Medline]
12. Rubio-Cabezas O, Puri V, Murano I, Saudek V, Semple RK, Dash S, *et al.* Partial lipodystrophy and insulin resistant diabetes in a patient with a homozygous nonsense mutation in CIDEC. EMBO Mol Med 2009;1: 280–7. [Medline]
13. Shlay JC, Sharma S, Peng G, Gibert CL, Grunfeld C, Terry Beirn Community Programs for Clinical

Research on AIDS (CPCRA), *et al.* The effect of individual antiretroviral drugs on body composition in HIV-infected persons initiating highly active antiretroviral therapy. J Acquir Immune Defic Syndr 2009;51: 298–304. [Medline]
14. Blümer RM, van Vonderen MG, Sutinen J, Hassink E, Ackermans M, van Agtmael MA, *et al.* Zidovudine/lamivudine contributes to insulin resistance within 3 months of starting combination antiretroviral therapy. AIDS 2008;22: 227–36. [Medline]
15. Shulman HM, Sullivan KM, Weiden PL, McDonald GB, Striker GE, Sale GE, *et al.* Chronic graft-versus-host syndrome in man. A long-term clinicopathologic study of 20 Seattle patients. Am J Med 1980;69: 204–17. [Medline]
16. Tanaka T, Yokoya S, Kato N, Ito Y, Tachibana K, Sugihara S, *et al.* Fundamental concept for the evaluation of Japanese children's physical constitution. J Jap Pediatr Soc 2011;115: 1705–9 (in Japanese).
17. Vigouroux C, Magré J, Vantyghem MC, Bourut C, Lascols O, Shackleton S, *et al.* Lamin A/C gene: sex-determined expression of mutations in Dunnigan-type familial partial lipodystrophy and absence of coding mutations in congenital and acquired generalized lipoatrophy. Diabetes 2000;49: 1958–62. [Medline]
18. Vantyghem MC, Vincent-Desplanques D, Defrance-Faivre F, Capeau J, Fermon C, Valat AS, *et al.* Fertility and obstetrical complications in women with LMNA-related familial partial lipodystrophy. J Clin Endocrinol Metab 2008;93: 2223–9. [Medline]
19. Haque WA, Shimomura I, Matsuzawa Y, Garg A. Serum adiponectin and leptin levels in patients with lipodystrophies. J Clin Endocrinol Metab 2002;87: 2395. [Medline]
20. Suganami T, Tanaka M, Ogawa Y. Adipose tissue inflammation and ectopic lipid accumulation. Endocr J 2012;59: 849–57. [Medline]
21. Misra A, Peethambaram A, Garg A. Clinical features and metabolic and autoimmune derangements in acquired partial lipodystrophy: report of 35 cases and review of the literature. Medicine (Baltimore) 2004;83: 18–34. [Medline]
22. Rooney DP, Ryan MF. Diabetes with partial lipodystrophy following sclerodermatous chronic graft vs. host disease. Diabet Med 2006;23: 436–40. [Medline]
23. Tomčík M, Arima K, Hulejová H, Kuklová M, Filková M, Braun M, *et al.* Adiponectin relation to skin changes and dyslipidemia in systemic sclerosis. Cytokine 2012;58: 165–8. [Medline]
24. Masui Y, Asano Y, Shibata S, Noda S, Aozasa N, Akamata K, *et al.* Serum adiponectin levels inversely correlate with the activity of progressive skin sclerosis in patients with diffuse cutaneous systemic sclerosis. J Eur Acad Dermatol Venereol 2012;26: 354–60. [Medline]
25. Ballesteros M, Leung KC, Ross RJ, Iismaa TP, Ho KK. Distribution and abundance of messenger ribonucleic acid for growth hormone receptor isoforms in human tissues. J Clin Endocrinol Metab 2000;85: 2865–71. [Medline]
26. Brent GA. Mechanisms of thyroid hormone action. J Clin Invest 2012;122: 3035–43. [Medline]
27. Corona G, Rastrelli G, Morelli A, Vignozzi L, Mannucci E, Maggi M. Hypogonadism and metabolic syndrome. J Endocrinol Invest 2011;34: 557–67. [Medline]
28. Jørgensen JO, Vestergaard E, Gormsen L, Jessen N, Nørrelund H, Christiansen JS, *et al.* Metabolic consequences of GH deficiency. J Endocrinol Invest 2005;28: 47–51. [Medline]
29. Tomita Y, Ishiguro H, Yasuda Y, Hyodo H, Koike T, Shimizu T, *et al.* High incidence of fatty liver and insulin resistance in long-term adult survivors of childhood SCT. Bone Marrow Transplant 2011;46: 416–25. [Medline]
30. Nuver J, Smit AJ, Postma A, Sleijfer DT, Gietema JA. The metabolic syndrome in long-term cancer survivors, an important target for secondary preventive measures. Cancer Treat Rev 2002;28: 195–214. [Medline]
31. Talvensaari KK, Lanning M, Tapanainen P, Knip M. Long-term survivors of childhood cancer have an increased risk of manifesting the metabolic syndrome. J Clin Endocrinol Metab 1996;81: 3051–5. [Medline]
32. Taskinen M, Saarinen-Pihkala UM, Hovi L, Lipsanen-Nyman M. Impaired glucose tolerance and dyslipidaemia as late effects after bone-marrow transplantation in childhood. Lancet 2000;356: 993–7. [Medline]
33. Shalitin S, Phillip M, Stein J, Goshen Y,

Carmi D, Yaniv I. Endocrine dysfunction and parameters of the metabolic syndrome after bone marrow transplantation during childhood and adolescence. Bone Marrow Transplant 2006;37: 1109–17. [Medline]

34. Smedmyr B, Wibell L, Simonsson B, Oberg G. Impaired glucose tolerance after autologous bone marrow transplantation. Bone Marrow Transplant 1990;6: 89–92. [Medline]
35. Nakanishi T, Li R, Liu Z, Yi M, Nakagawa Y, Ohzeki T. Sexual dimorphism in relationship of serum leptin and relative weight for the standard in normal-weight, but not in overweight, children as well as adolescents. Eur J Clin Nutr 2001;55: 989–93. [Medline]
36. Takahara M, Katakami N, Kishida K, Kaneto H, Funahashi T, Shimomura I, *et al.* Circulating adiponectin levels and their associated factors in young lean healthy Japanese women. J Atheroscler Thromb 2013;20: 57–64. [Medline]
37. Ogawa Y, Kikuchi T, Nagasaki K, Hiura M, Tanaka Y, Uchiyama M. Usefulness of serum adiponectin level as a diagnostic marker of metabolic syndrome in obese Japanese children. Hypertens Res 2005;28: 51–7. [Medline]

CLINICAL REPORT

AMERICAN JOURNAL OF medical genetics PART A

# First Case of a Japanese Girl With Myhre Syndrome Due to a Heterozygous *SMAD4* Mutation

**Yumi Asakura,[1]* Koji Muroya,[1] Takeshi Sato,[1] Kenji Kurosawa,[2] Gen Nishimura,[3] and Masanori Adachi[1]**

[1]Department of Endocrinology and Metabolism, Kanagawa Children's Medical Center, Mutsukawa, Minami-ku, Yokohama-shi, Kanagawa, Japan

[2]Department of Genetics, Kanagawa Children's Medical Center

[3]Department of Pediatric Imaging, Tokyo Metropolitan Children's Medical Center, Musashidai, Fuchu-shi, Tokyo, Japan

Manuscript Received: 7 March 2012; Manuscript Accepted: 1 April 2012

This article reports the first case of a Japanese girl with molecularly confirmed Myhre syndrome (MS). The patient was 9 years old at her first visit, and she had been diagnosed with unknown skeletal dysplasia. Her phenotype fulfilled the clinical and radiological criteria for MS, such as typical facies with prognathism, hearing impairment, short stature, square body shape, and limited joint mobility. The thick calvarium and thick skin were clues to the clinical diagnosis of MS. A heterozygous mutation in the mothers-against-DPP homolog 4 (*SMAD4*) gene has been reported to cause MS. We sequenced *SMAD4* using standard PCR-based technique and identified a recurrent mutation (p.Ile500 Thr). She attained menarche before 11 years of age; however, she developed oligomenorrhea after a few years of 40-day cycles, necessitating hormone replacement therapy. The luteinizing hormone-releasing hormone (LHRH) tests suggested abnormalities related to hypothalamo-hypophyseal malfunction. Previous reports on MS described early menarche in girls and early or delayed puberty and cryptorchidism in boys. Therefore, we recommend performing an endocrinological evaluation of the hypothalamo-hypophyseal-gonadal axis in patients with MS to clarify whether hormonal abnormalities are associated with the syndrome. 

**Key words:** Myhre syndrome; *SMAD4*; growth retardation; thick calvarium; muscular hypertrophy; gonadal dysfunction

**How to Cite this Article:**
Asakura Y, Muroya K, Sato T, Kurosawa K, Nishimura G, Adachi M. 2012. First case of a Japanese girl with Myhre syndrome due to a heterozygous *SMAD4* mutation.
Am J Med Genet Part A 158A:1982–1986.

## INTRODUCTION

Myhre syndrome (MS, OMIM 139210) is a rare connective tissue disorder and was first described by Myhre et al. [1981] in two unrelated males in 1981. Since then, fewer than 30 individuals with MS have been reported till date [Soljak et al., 1983; Garcia-Cruz et al., 1993; Titomanlio et al., 2001; Whiteford et al., 2001; Burglen et al., 2003; Dávalos et al., 2003; Lopez-Cardona et al., 2004; Rulli et al., 2005; Van Steensel et al., 2005; Becerra-Solano et al., 2008]. The clinical hallmarks of MS include intellectual disability; low birth weight; poor postnatal growth leading to short stature; conductive and sensorial hearing loss; muscular hypertrophy; limited joint mobility; and typical facies characterized by distinct prognathism, blepharophimosis, and a narrow mouth. X-ray findings of MS include a thick calvarium, mandibular protrusion, mild rib broadening, hypoplastic iliac wings, shortening of the tubular bones, and somewhat flattened vertebral bodies with large, short pedicles. Two recent studies have carried out exome sequencing of individuals with MS and reported that heterozygous missense mothers-against-decapentaplegic homolog of 4 (*SMAD4*; NM 005359) mutations affect the codon for Ile500 in all the study subjects (n = 19) [Caputo et al., 2012; Le Goff et al., 2012]. We sequenced the *SMAD4* gene using standard PCR-based technique and identified a recurrent mutation (p.Ile500 Thr) in our patient. Early menarche in girls and early or delayed puberty and cryptorchidism in boys have been reported in MS. Our patient also complained of oligomenorrhea. In this article, we report on a case of molecularly confirmed MS and hormonal evaluations of the patient.

## CLINICAL REPORT

We obtained written informed consent from the patient and her parents for molecular studies and publication of her clinical

Additional supporting information may be found in the online version of this article.

Conflicts of interest: None.

*Correspondence to:
Yumi Asakura, M.D., Department of Endocrinology and Metabolism, Kanagawa Children's Medical Center, 2-138-4 Mutsukawa, Minami-ku, Yokohama-shi, Kanagawa 232-8555, Japan.
E-mail: yumi79@mvb.biglobe.ne.jp

Article first published online in Wiley Online Library (wileyonlinelibrary.com): 18 June 2012
DOI 10.1002/ajmg.a.35440